

Synthesis and Evaluation of the Cytotoxicities of Tetraindoles: Observation that the 5-Hydroxy Tetraindole (SK228) Induces G₂ Arrest and Apoptosis in Human Breast Cancer Cells

Wen-Shan Li,^{*,†,§} Chie-Hong Wang,^{†,‡,#} Shengkai Ko,^{†,||,#} Tzu Ting Chang,[†] Ya Ching Jen,[†] Ching-Fa Yao,^{*,||} Shivaji V. More,[†] and Shu-Chuan Jao[⊥]

[†]Institute of Chemistry, Academia Sinica, Taipei 115, Taiwan

[‡]Institute of Biomedical Sciences, National Sun Yat-Sen University, Kaohsiung 804, Taiwan

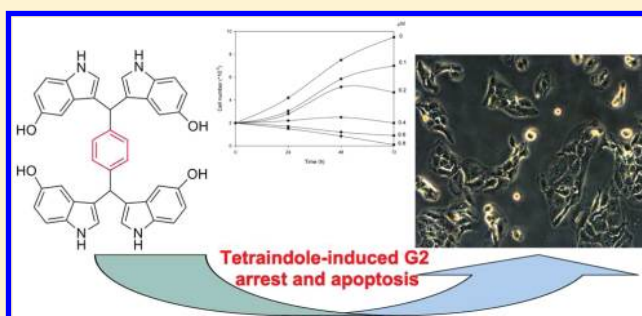
[§]Doctoral Degree Program in Marine Biotechnology, National Sun Yat-Sen University, Kaohsiung 804, Taiwan

^{||}Department of Chemistry, National Taiwan Normal University, Taipei 116, Taiwan

[⊥]Institute of Biological Chemistry, Academia Sinica, Taipei 115, Taiwan

Supporting Information

ABSTRACT: Current chemical and biological interest in indole-3-carbinol (I3C) and its metabolites has resulted in the discovery of new biologically active indoles. As part of a program aimed at the development of indole analogues, tetraindoles 1–15 were prepared and their antiproliferative effects on human breast cancer cells were evaluated. The results show that the 5-hydroxy-tetraindole 8 (SK228) has optimum antiproliferative activity against breast adenocarcinoma (MCF 7 and MDA-MB-231) cells and that this activity involves G₂-phase arrest of the cell cycle with a distinctive increase in the expression of cyclin B1 and phospho-cdc2. Further observations suggest that 5-hydroxy-tetraindole 8 induces apoptosis through externalization of membrane phosphatidylserine, DNA fragmentation, and activation of caspase-3. Given the fact that I3C and its metabolites have been shown to improve therapeutic efficacy and to have a broad range of antitumor activities in human cancer cells, the current findings have important pharmacological relevance as they open a promising route to the development of a potential chemotherapeutic application of tetraindoles as agents for the treatment of breast cancer.



INTRODUCTION

The utility of indoles, such as indole-3-carbinol (I3C),¹ 3,3'-diindolylmethane (DIM),² indole-3-carbinol cyclic trimer CTr,³ and cyclic tetramer CTet⁴ (Chart 1), as chemopreventive and chemotherapeutic agents has recently been recognized. Indole-3-carbinol (I3C) is a dietary compound and an autolysis product of glucosinolate (glucobrassicin), which was identified and isolated from *Brassica* vegetables such as cabbage, broccoli, and Brussels sprouts. The results of epidemiological and dietary studies continue to demonstrate that high dietary intake of cruciferous vegetables can prevent carcinogenesis.⁵ Moreover, I3C, DIM, and CTet are known to exhibit a broad spectrum of antiproliferative effects on various tumors (e.g., breast, colon, prostate, and endometrial cancers) with effective concentrations in the range of 1–100 μ M.^{1–4,6} Unlike I3C and its stomach digest products (DIM and CTet), the cyclic trimer CTr functions by stimulating the proliferation of estrogen-responsive MCF-7 cells that contributes to the overall estrogenic effect of oral I3C.^{4c}

The exact mechanism(s) of I3C and DIM mediated suppression of cancer growth remains under studied. It is

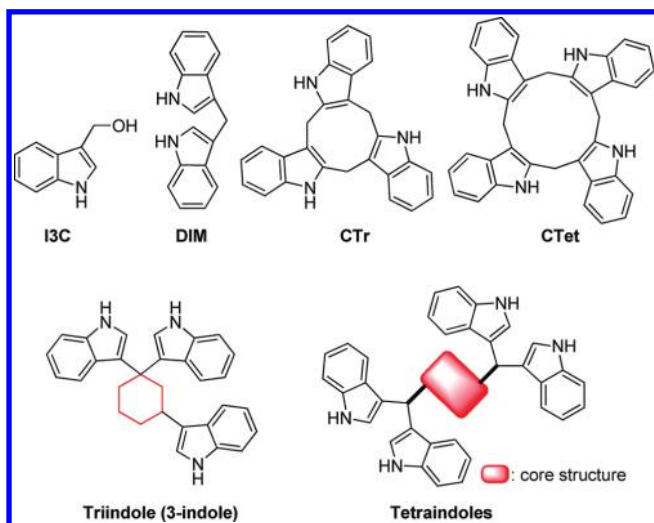
highly likely that multiple mechanisms (e.g., Akt-NF κ B signaling, caspase activation, cyclin-dependent kinase activity, estrogen receptor signaling, endoplasmic reticulum stress, and BRCA gene expression) are operating in different proportions under different conditions within various cell types.^{1–4,7} In contrast, therapeutic applications based on CTet have developed only slowly. Although I3C has been studied in the context of cancer prevention in preclinical trials,⁵ it is not readily amenable to general systemic therapeutic purposes owing to its poor efficacy and unacceptable pharmacokinetic properties.⁸ In the stomach, gastric acids convert the inactive prodrug I3C into the pharmacologically active metabolites DIM, CTet, or other indole oligomers that possess in vivo antitumor activity.^{1–4}

Because they serve as potential chemical building blocks for construction of different I3C-related antitumor agents employed in demonstrated apoptotic pathways, indoles have garnered considerable medicinal interest. For example, a variety

Received: October 7, 2011

Published: January 25, 2012

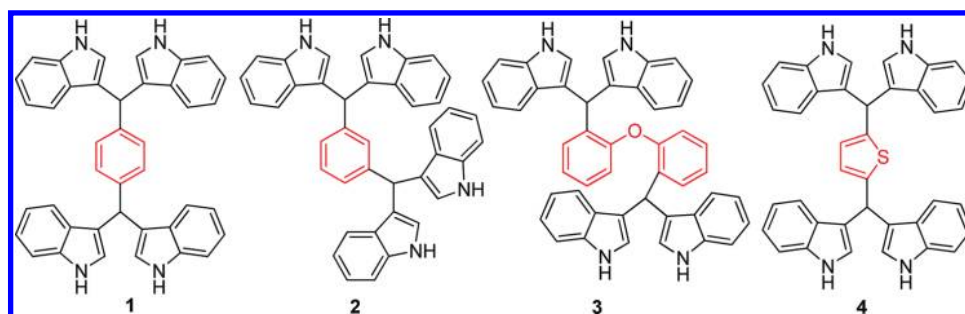
Chart 1



of structurally diverse synthetic indole-based compounds, such as BPROL075,⁹ I-387,¹⁰ NSC-741909,¹¹ SR13668,¹² NB-506,¹³ OSU-A9,¹⁴ ES936,¹⁵ EO9,¹⁶ KW-2189,¹⁷ and their analogues, display tumor growth inhibition against a wide range of cancer cell lines and effective antitumor activities in various preclinical models. We have recently demonstrated that 3-indole (triindole or 1,1,3-tri[3-indolyl]cyclohexane; Chart 1), possessing a cyclohexane core structure, induces apoptosis in various lung cancer cells and xenograft models.¹⁸ The apoptosis results from an intrinsic mitochondrial pathway involving stress-activated pathways, including reactive oxygen species (ROS) and c-Jun N-terminal kinase (JNK) activities.¹⁸

In the study described below, we designed and synthesized a series of tetraindole analogues (Chart 2), derived from the 3-indole platform, and explored their therapeutic effects against breast cancer cells. Special interest focused on the identification of central core structures (benzene, oxidibenzene, or thiophene in Chart 2), which would support biological activity and whose substructure optimization would effectively produce substances with high antitumor activities. In this effort, 5-hydroxy tetraindole **8** (SK228)¹⁹ was identified as a potential strong lead compound based on its effectively therapeutic action, with IC_{50} values falling in the nanomolar range. Observations made in the investigation suggest that **8** (SK228) mediates G_2 -phase arrest along with apoptosis involving the intrinsic pathway. The findings lead to a new paradigm for the pharmacological use of tetraindoles in the treatment of human breast cancer.

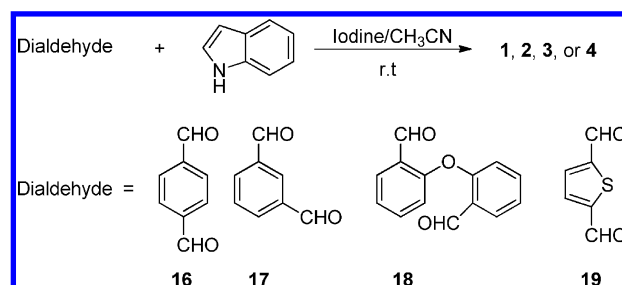
Chart 2



RESULTS AND DISCUSSION

Design and Synthesis. Tetraindoles **1–4** (Chart 2), bearing an aromatic central core structure, were prepared in satisfactory yields by addition reactions of various dialdehydes **16–19** with indole in the presence of catalytic amounts of molecular iodine at room temperature (Scheme 1).²⁰ By

Scheme 1

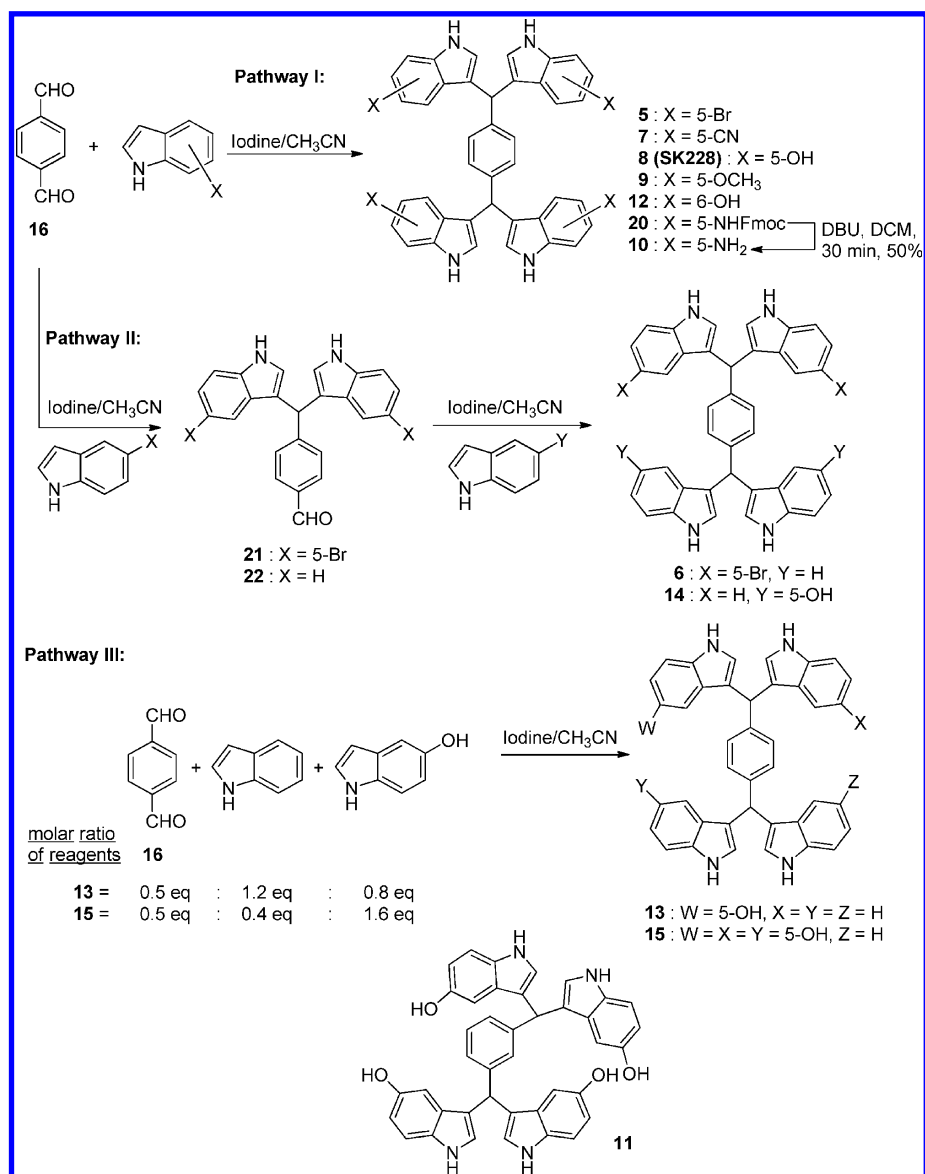


employing this strategy, tetraindole **1** analogues **5**, **7–9**, **12**, and **20** were synthesized by reacting terephthalaldehyde **16** with various substituted indoles under the same condition (Scheme 2, pathway I). Sequential removal of the Fmoc group of **20** gave **10**. Tetraindole **11**, where the central core structure is replaced by a 2,2'-oxybisbenzene, was synthesized starting with isophthalaldehyde (**17**) and 5-hydroxyindole.

Electron-withdrawing (Br) and electron-donating groups (OH), were introduced at the C-5 position of the indole ring to generate unsymmetrical tetraindoles **6** and **14**, prepared as outlined in Scheme 2 (pathway II). Under similar conditions, the intermediate aldehydes **21** and **22** could be isolated and undergo reactions catalyzed by molecular iodine to afford the respective unsymmetrical tetraindoles **6** and **14**. In contrast, the unsymmetrical mono-5-hydroxyindole **13** and tri-5-hydroxyindole **15** were prepared by iodine-catalyzed addition reactions of terephthalaldehyde (**16**) with different molar ratio of indole and 5-hydroxyindole (Scheme 2, pathway III). It should be noted that the studies described above resulted in the development of a new strategy to prepare unsymmetrical tetraindoles in high yields.

Growth Inhibition by Tetraindoles against Human Breast Cancer Cells. Inspired by the results of previous studies of 3-indole in lung cancer¹⁸ and the antiproliferative effects of 3-indole and its digestion products on breast cancer cells (Table 1),^{1–4} we postulated that an increase in the number of active indole rings in a substance would facilitate its cell cytotoxicity and, hence, its inhibition of tumor cell growth in vitro. As a first step in exploring this proposal, we designed and prepared new tetraindoles **1–4** (Chart 2), bearing different

Scheme 2



central core structures (e.g., benzene, oxidibenzene, or thiophene), and evaluated their antiproliferative activities against human breast cancer cells using an MTT assay. The results show that unlike 3 and 4, which exhibit less potent effects against MDA-MB-231, 1 and 2, possessing the respective 1,4-benzene and 1,3-benzene core structural units, display improved growth-inhibitory potency with respective IC₅₀ values of 9.8 and 24.3 μM (Table 1). Furthermore, in comparison to the other tetraindoles, 1 displays a high potency toward MCF 7 breast adenocarcinoma cells (16.1 μM). These observations indicate that a benzene rather than oxidibenzene/thiophene core structures are required for antiproliferative activities of tetraindoles against breast cancer cells.

Building on these observations, six new tetraindoles 5–10, having a benzene core structure and electron-withdrawing (Br and CN) and electron-donating groups (OH, OCH₃, and NH₂) at C-5 positions of their indole rings, were prepared. Among these substances, 8 was observed to have the highest antiproliferative activity, with IC₅₀ values of 0.45–0.88 μM against two human breast cancer cell lines, which are 18–45-fold lower than those of 1 and 3-indole (Table 1). Notably, the

antiproliferative effect of 8 is 2–57 times more potent than those of the well-known I3C metabolites, DIM and CTet (Table 1). In contrast, the five other tetraindoles 5–7, 9, and 10 display no apparent effects on MDA-MB-231 cell growth at 20 μM concentrations. To our surprise, tetraindoles 5, 6, 9, and 10, bearing respective 5-bromo, -methoxy, and -amino substituents on the indole ring, also display dramatically decreased antiproliferative effects toward MCF-7 cells. It is important to note that the 5-cyano tetraindole 7 is 2-fold more potent (IC₅₀ = 9.5 μM) than 1 (Table 1). Interestingly, the relative IC₅₀ values of 7 show dissimilar trends against the ER+ cell line MCF-7 and ER– cell line MDA-MB-231, an observation that indicates that the effects on cell growth inhibition might be caused by an effect on an estrogen receptor (ER)-dependent pathway.

In the series explored, 8, possessing a hydroxy group at the indole C-5 position, was found to be the most active compound against MDA-MB-231 and MCF-7 (Table 1), suggesting that the introduction of hydroxy substituents into position 5 on each indole ring would favor cancer cell growth inhibition. Indeed, tetraindole 11, bearing a hydroxy group at the C-5

Table 1. Growth Inhibitory Activity of Tetraindoles Against Breast Cancer Cells^a

compd	MDA-MB-231	MCF-7
DIM ⁶	10–20	50.0 ± 8.0
CTet ⁴	1.0 ± 0.1	1.3 ± 0.1 or 8.0 ± 0.5
3-indole	20.1 ± 2.2	19.8 ± 1.6
1	9.8 ± 1.7	16.1 ± 0.6
2	24.3 ± 3.5	>20 (32) ^b
3	>20 (8) ^b	>20 (48) ^b
4	>20 (36) ^b	>20 (34) ^b
5	>20 (5) ^b	>20 (25) ^b
6	>20 (8) ^b	>20 (17) ^b
7	>20 (8) ^b	9.5 ± 0.9
8	0.45 ± 0.03	0.88 ± 0.04
9	>20 (3) ^b	>20 (43) ^b
10	>20 (35) ^b	>20 (25) ^b
11	>20 (0) ^b	17.8 ± 3.7
12	>20 (16) ^b	>20 (0) ^b
13	13.9 ± 1.6	12.6 ± 1.3
14	>20 (36) ^b	>20 (23) ^b
15	7.8 ± 0.6	6.3 ± 0.7

^aAmount of drug and tetraindoles **1–15** necessary to inhibit the growth of breast cancer cells (MCF-7 and MDA-MB-231) by 50% in 48 h. Data are means ± SD (*n* = 3). ^bThe percent (%) inhibition, in parentheses, at 20 μM is expressed as the percent (%) inhibition of cell growth.

position of each indole ring connected to the 1,3-benzene core structure, was found to have an improved growth-inhibitory potency (IC₅₀ = 17.8 μM) against MCF-7 as compared to the parent compound **2**. However, the introduction of a hydroxy group at the C-6 position of the indole ring as in **12**, results in dramatically decreased potency compared to that of **8** toward two breast cancer cell lines. This observation suggests that the location of a hydroxy group at C-5 rather than C-6 on each indole ring is important in bringing about suppression of breast cancer cell growth.

The variation in the number of hydroxy groups of **8** raises an intriguing question about whether or not there is a biological divergence altering the presence or absence of C-5 hydroxy group in tetraindoles. The relative order of antiproliferative potency of **8** analogues is **8** (four hydroxy groups) > **15** (three hydroxy groups) > **13** (one hydroxy group) ≫ **14** (two hydroxy groups), implying that modifications of the total number of 5-hydroxy groups affect the ability of tetraindoles to modulate antiproliferative potency. The at least 7–44-fold weaker potency of tetraindoles **13–15**, compared with **8**, supports this suggestion.

Compound 8 Decreases the Survival Rate of MDA-MB-231 and Inhibits the Cells' Growth of a Variety of Cancer Cell Lines. A greater understanding of the mechanistic source of the growth inhibitory effects of **8** should provide insight into its mode of biological action and aid the design of more effective antitumor agents. In the conventional MTT assay, **8** was found to inhibit MDA-MB-231 cell viability (IC₅₀ = 0.45 μM) in a dose-dependent manner (Supporting Information Figure S1). A similar effect was observed in MCF-7 cells (data not shown), indicating that MDA-MB-231 is more sensitive to **8**-induced cell growth inhibition than is MCF-7 (IC₅₀ = 0.88 μM). The antiproliferative effect of **8** on MDA-MB-231 cells was also examined by using the trypan blue dye

exclusion method.²¹ Cells were treated with increasing concentrations of **8** (0–800 nM) at 24, 48, and 72 h, respectively (Figure 1). The results demonstrate that **8**

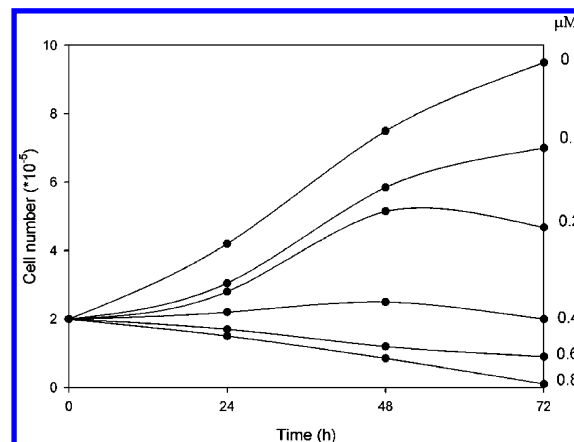


Figure 1. Time- and dose-dependent antiproliferation effect of **8** (DMSO vehicle; 0.1, 0.2, 0.4, 0.6, 0.8 μM) on MDA-MB-231 cells. Cells were plated at a density of 200000 cells per well in 6-well culture plates and treated with the different concentrations of **8** in 10% FBS-supplemented DMEM/F12 medium. At different time intervals, cells were harvested by trypsinization and counted using a hemocytometer. The values plotted are representative of three independent experiments.

treatment significantly suppresses cell proliferation of MDA-MB-231 cells and decreases the cell count in both a time and dose-dependent manner. This result is in line with the previous observations.¹⁹

In addition, *in vitro* antiproliferative activities of **8** against a panel of human cancer cell lines, including MDA-MB-361 (breast adenocarcinoma), MDA-MB-468 (breast adenocarcinoma), SW480 (colon adenocarcinoma), SW620 (colon adenocarcinoma), SW48 (colon adenocarcinoma), U-87 MG (glioblastoma), and A549 (lung adenocarcinoma), were determined (Table 2). **8** was found to exhibit similar or greater growth inhibitory activities against seven human cancer cell lines (Supporting Information Figures S2–S8) compared to MCF-7 and MDA-MB-231 cell lines. It is interesting to note that **8** shows significant inhibition against the SW480 cancer cell line.

Building on these cytotoxicity results, we extended studies to evaluate the selectivity of **8** for malignant versus normal cells (breast epithelium cell line, M10, and skin embryo fibroblast, Detroit 551). Selective cytotoxicity against tumor rather than normal cells is an important factor determining the usefulness of anticancer agents in the treatment of cancer. As the data in Tables 1 and 2 show, **8** displays cytotoxicity against nine human cancer cell lines with IC₅₀ values ranging from 0.37 to 2.89 μM, and shows a lower activity (2–54-fold less cytotoxic) against two normal cell lines, with IC₅₀ values ranging from 5.81–20.0 μM. These findings indicate that **8** displays a differential selectivity for tumor over normal cells (Supporting Information Figures S9 and S10).

Compound 8 Induces G₂ Phase Arrest. To determine whether the suppression of breast cancer cell growth by **8** is caused by a cell cycle effect, MDA-MB-231 cells were cultured with 800 nM **8** for 24 and 48 h, respectively, and cell cycle progression was evaluated by using flow cytometry. The analysis with MDA-MB-231 cells indicates that the number of

Table 2. Growth Inhibitory Activity of **8** against Seven Cultured Human Tumor Cell Lines^a

compd	IC ₅₀ (μM)								
	MDA-MB-361	MDA-MB-468	SW480	SW620	SW48	U-87 MG	A549	M10	Detroit 551
8	2.07 ± 0.11	0.83 ± 0.06	0.37 ± 0.05	0.98 ± 0.02	0.88 ± 0.05	2.73 ± 0.35	2.89 ± 0.25	5.81 ± 0.28	>20 (47) ^b

^aAmount of **8** necessary to inhibit the growth of a panel of human cancer cells by 50% in 48 h. Data are means ± SD (*n* = 3). ^bThe percent (%) inhibition, in parentheses, at 20 μM is expressed as the percent (%) inhibition of cell growth.

cells in the G₂/M phase increases from 30% in a control to 40% and G₂/M arrest is accompanied by a concomitant decrease in G₁-phase cells (48–31%) at 24 h (Figure 2). In comparison, **8**

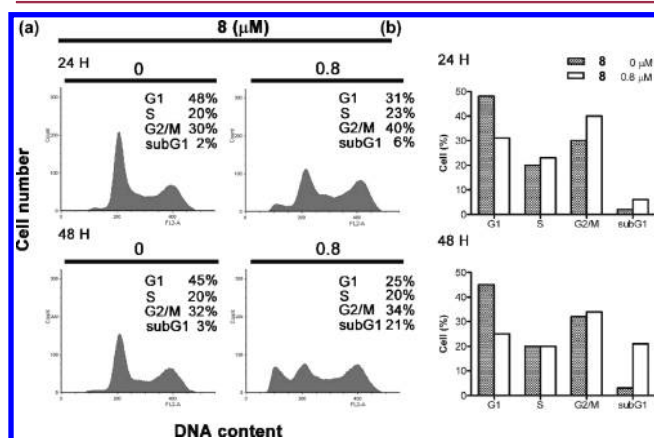


Figure 2. Effect of **8** on cell cycle distribution of MDA-MB-231 breast cancer cells. (a) FACS analysis of the cell cycle. MDA-MB-231 cells were treated with DMSO (vehicle control) or 0.8 μM **8** and incubated for 24 and 48 h, respectively. Cells were then stained with propidium iodide and analyzed for DNA content by using flow cytometry. A total of 25000 cells were analyzed from each sample. (b) Graph bars show the distributions at different portions of the cell cycle at 24 and 48 h.

treated cells display a substantial increase at 48 h in the sub-G₁ region, indicated as apoptotic cells (3–21%). Together, these results demonstrate that **8** treated breast cancer cells are arrested in G₂/M phase before cell death occurs.

It has been shown previously that cyclin B1, in association with the cdc2 kinase (known as cdk1), regulates cell cycle progression from the G₂ to the M phase.²² This observations explains why G₂/M arrest is associated with overexpression of cyclin B1.²³ Phosphorylation of Tyr15 of cdc2 is observed to inactivate cdc2 kinase and suppress activity of the cdc2–cyclin B1 complex, which remains in the cytoplasm rather than in the nucleus (only active form of cdc2–cyclin B1 complex).²⁴

To gain insight into the molecular mode of action involved in G₂/M arrest, the effect of **8** on the mitosis promoting factors, cyclin B1 and phospho-cdc2, was investigated using Western blot analysis (Figure 3). Expression levels of cyclin B1 and phospho-cdc2 were observed to significantly increase upon treatment with **8** in a dose-dependent manner for 24 and 48 h. This observation of a high phospho-cdc2 level suggests that both the activity and level of cdc2–cyclin B1 complex decrease. Hence, complete termination of the progression of the cells to mitosis is likely, indicating that **8**-treated MDA-MB-231 cells are arrested in the G₂ phase but not the M phase. A low cyclin B1 level was also observed after only 48 h treatment with the highest concentration (0.8 μM) of **8**, suggesting perhaps that MDA-MB-231 cells are in late apoptosis or cell death. This observation is in excellent agreement with detection of sub-G₁

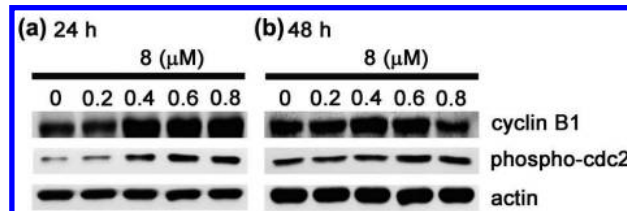


Figure 3. **8**-induced alterations in cell cycle G₂/M phase regulatory genes. Western blot analysis of cyclin B1 and phospho-cdc2(Tyr¹⁵) in MDA-MB-231 cells treated with indicated concentrations of **8**. Actin was probed as an internal control.

cell population (Figure 2) and later data from an annexin V-FITC/propidium iodide (PI) binding assay (Figure 4).

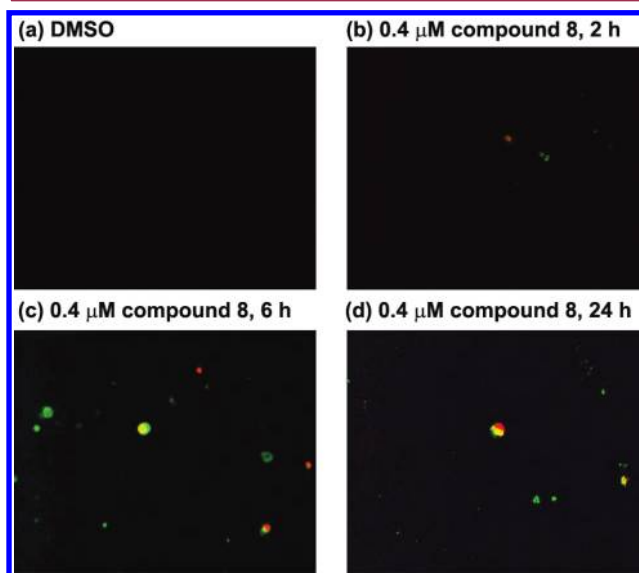


Figure 4. Fluorescence microscopy analysis of apoptosis. MDA-MB-231 cells were treated with indicated concentrations of **8** in different time intervals. After treatment, cells were washed twice with PBS then followed by the commercial kit user's guide (normal cells, annexin V negative and PI negative; early apoptotic cells, annexin V positive and PI negative; late apoptotic cells, annexin V positive and PI positive).

Compound **8 Induces Apoptosis.** To better understand whether the loss of cancer cell viability promoted by **8** is associated with apoptosis, an annexin V-FITC/propidium iodide (PI) binding assay was performed. Because annexin V-FITC has a high, Ca²⁺-dependent affinity for phosphatidylserine (PS) residues, the elements of phospholipid on the inner leaflet locations of PS residues are easily externalized during the progression of apoptosis. Three cell populations, including viable (annexin V-FITC, negative; PI, negative), early apoptotic (annexin V-FITC, positive; PI, negative), and late apoptotic cells or dead cells (annexin V-FITC, positive; PI, positive), were utilized for this purpose. After treatment with 0.4 μM **8**, early (annexin V-FITC, positive; PI, negative) and late

apoptosis (annexin V-FITC, positive; PI, positive) take place with MDA-MB-231 cells in a time-dependent manner (Figure 4b–d), indicating that **8** induces significant apoptotic cell death in MDA-MB-231 cells.

To further confirm that **8**-induced formation of a sub- G_1 peak is associated with apoptosis, experiments probing DNA ladder formation were carried out. As the images in in Figure 5

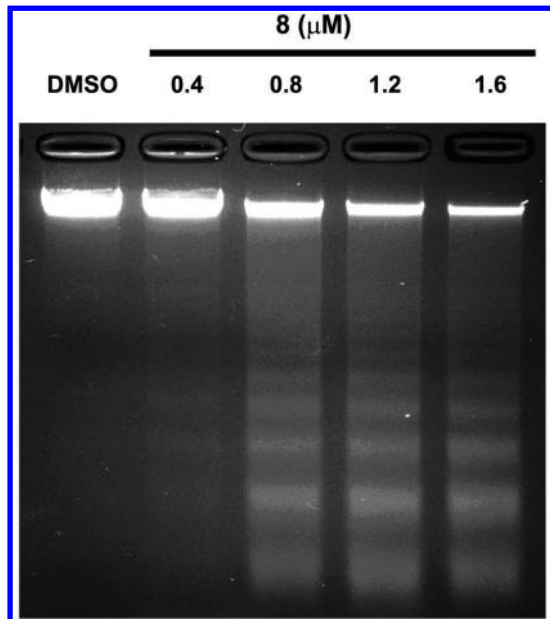


Figure 5. Activation of apoptosis by **8** in MDA-MB-231 cells. DNA ladder formation in MDA-MB-231 cells treated with 0, 0.4, 0.8, 1.2, and 1.6 μM **8** for 48 h.

show, treatment of MDA-MB-231 cells with different concentrations of **8** (0.4, 0.8, 1.2, and 1.6 μM) causes formation of an apoptotic DNA ladder pattern.

Two major mechanisms for the induction of apoptosis exist, including one that follows an extrinsic apoptotic pathway and the other following an intrinsic apoptotic pathway.²⁵ The results of a few recent studies show that indole and its analogues commonly induce apoptosis by the intrinsic pathway involving the modulated expression of the apoptotic regulatory proteins, bcl-2/bak. Therefore, in an effort to examine the expression levels of apoptosis-related proteins (Figure 6), we

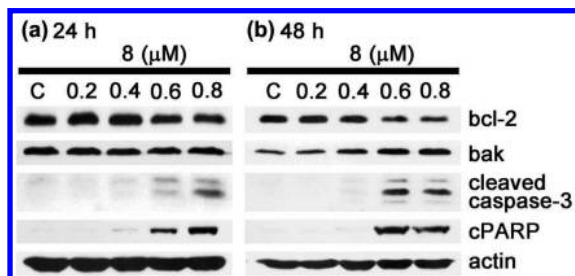


Figure 6. **8**-induced apoptosis in MDA-MB-231 cells. Western blot analysis of bcl-2, bak, cleaved caspase-3, and cleaved PARP (cPARP) in MDA-MB-231 cells treated with indicated concentrations of **8**. Actin was probed as an internal control.

observed that treatment of MDA-MB-231 cells with different concentrations of **8** decreases bcl-2 (antiapoptotic protein) protein levels in a dose-dependent manner. However, **8** was

found to increase bak (pro-apoptotic protein) levels simultaneously at 24 and 48 h. This finding is consistent with well-documented observations that blockage of Bcl-2 levels and activation of bak proteins are essential steps in the intrinsic apoptotic pathway.²⁶ Furthermore, the result of a Western blot experiment also demonstrates that **8** causes a dose-dependent increase in protein levels of cleaved caspase-3 and cleavage of poly(ADP-ribose)polymerase (cPARP) (Figure 6). Taken together, the results suggest that perhaps **8** induced apoptosis follows the intrinsic mitochondrial pathway.

CONCLUSIONS

Because of the widespread chemopreventive and chemotherapeutic applications of I3C and its metabolites, a strong demand exists for an efficient strategy to search for other pharmacologically active indole analogues. The findings arising from the studies described above open a possible approach to the design and development of new indole analogues, such as tetraindoles, that serve as anticancer agents for the treatment of human breast cancer. In this effort, we have identified **8** as a potent, nanomolar range anticancer agent against MDA-MB-231 and MCF-7 cells. This substance mediates G_2 -phase arrest via up-regulation of cyclin B1 and phospho-cdc2 and induces apoptosis involving the intrinsic pathway. Further investigations to sensitize breast cancer cells to the actions of **8** are underway.

EXPERIMENTAL SECTION

Chemistry. All chemicals and reagents were commercially available and used without further purification unless indicated otherwise. All solvents were anhydrous grade unless indicated otherwise. Reactions were monitored by using thin-layer chromatography on silica gel. Flash chromatography was performed on silica gel of 60–200 μm particle size. NMR spectra were recorded on Bruker AMX400, AV300, AV400, or AV500 MHz instruments. Chemical shifts were reported in ppm and are referenced to the chemical shift of residual solvent. High resolution mass spectra were recorded on a Bruker Daltonics spectrometer. Chromatography was performed at room temperature using a high-performance liquid chromatography (HPLC) consisting of a Waters model 501 single pump system with a Merck Si-60 (25 cm \times 10 cm) column equilibrated in hexane/EtOAc or methanol as eluents, at a flow rate of 2 mL/min, and the eluted materials were monitored using a UV absorbance detector that measured the absorbance at 254 nm, unless indicated otherwise. The HPLC fractions containing products were dried in a vacuum concentrator (Speedvac SC110, Savant Instruments, Holbrook, NY). The purity of the tetraindoles was established as being >95% by employing HPLC and ^1H NMR.

Representative Procedure for the Synthesis of Tetraindoles 1, 5, 7–9, and 12: 1,4-Bis(di(1H-indol-3-yl)methyl)benzene (1).

A round-bottomed flask (10 mL) was charged with terephthalaldehyde (0.13 g, 1.0 mmol), substituted indole (4 mmol), and iodine (0.025 g, 0.1 mmol) in ether or MeCN (1 mL). This mixture was then stirred for 2 h at room temperature. The reaction mixture was treated with aqueous $\text{Na}_2\text{S}_2\text{O}_3$, and the solution was extracted with ethyl acetate (2 \times 20 mL). The combined organic layers were dried over MgSO_4 and filtered. The solvent was removed under reduced pressure, and the residue was subjected to flash column chromatography, followed by normal-phase HPLC to afford the pure product as a powder (93%), mp 183–184 $^\circ\text{C}$. ^1H NMR (400 MHz, CDCl_3) 7.38–7.35 (m, 8H), 7.25–7.21 (m, 8H), 7.14 (td, $J = 6.9, 1.1$ Hz, 4H), 7.01 (td, $J = 7.0, 1.0$ Hz, 4H), 6.25–6.23 (m, 4H), 5.75 (s, 2H). ^{13}C NMR (100 MHz, CDCl_3) 141.6, 136.7, 128.6, 127.1, 123.6, 121.8, 120.0, 119.7, 119.0, 111.1, 39.9. HRMS calcd for $\text{C}_{40}\text{H}_{30}\text{N}_4$ (M^+), 566.2470; found, 566.2469.

Representative Procedure for the Synthesis of Tetraindoles 2 and 11: 1,3-Bis(di(1H-indol-3-yl)methyl)benzene (2). A round-bottomed flask (10 mL) was charged with isophthalaldehyde (0.13 g,

1.0 mmol), 5-substituted indole (4 mmol), and iodine (0.025 g, 0.1 mmol) in ether or MeCN (1 mL). This mixture was then stirred for 2 h at room temperature. The reaction mixture was treated with aqueous $\text{Na}_2\text{S}_2\text{O}_3$, and the solution was extracted with ethyl acetate (2×20 mL). The combined organic layers were dried over MgSO_4 and filtered. The solvent was removed under reduced pressure, and the residue was subjected to flash column chromatography, followed by normal-phase HPLC to afford the pure product as a powder (91%), mp 165–166 °C. ^1H NMR (400 MHz, CDCl_3) 7.34 (d, $J = 7.9$ Hz, 4H), 7.16–7.06 (m, 16H), 7.00 (t, $J = 7.4$ Hz, 4H), 5.99 (s, 4H), 5.68 (s, 2H). ^{13}C NMR (100 MHz, CDCl_3) 143.9, 136.5, 129.3, 128.2, 127.0, 126.6, 123.5, 121.7, 120.0, 119.4, 119.0, 111.1, 40.3. HRMS calcd for $\text{C}_{40}\text{H}_{30}\text{N}_4$ (M^+), 566.2470; found, 566.2471.

Representative Procedure for the Synthesis of Tetraindole 3: 3,3',3'',3'''-(2,2'-Oxybis(2,1-phenylene)bis(methanetriyl)tetrakis(1H-indole)) (3). A round-bottomed flask (10 mL) was charged with 2,2'-oxidibenzaldehyde (0.23 g, 1.0 mmol), indole (0.47 g, 4 mmol), and iodine (0.025 g, 0.1 mmol) in ether (1 mL). This mixture was then stirred for 2 h at room temperature. The reaction mixture was treated with aqueous $\text{Na}_2\text{S}_2\text{O}_3$, and the solution was extracted with ethyl acetate (2×20 mL). The combined organic layers were dried over MgSO_4 and filtered. The solvent was removed under reduced pressure, and the residue was subjected to flash column chromatography, followed by normal-phase HPLC to afford the pure product as a powder (93%), mp 169–170 °C. ^1H NMR (400 MHz, CDCl_3) 7.28 (d, $J = 8.0$ Hz, 4H), 7.23 (dd, $J = 7.6, 1.6$ Hz, 2H), 7.14–7.06 (m, 12H), 7.06–7.01 (m, 2H), 6.93–6.84 (m, 6H), 6.67 (d, $J = 8.0$ Hz, 2H), 6.28 (br s, 4H), 6.06 (s, 2H). ^{13}C NMR (100 MHz, CDCl_3) 155.5, 136.7, 134.6, 130.2, 127.6, 127.2, 124.1, 123.0, 121.7, 120.2, 119.1, 118.5, 111.3, 34.4, 34.4. HRMS calcd for $\text{C}_{46}\text{H}_{33}\text{N}_4\text{O}$ ($\text{M} - \text{H}$), 657.2655; found, 657.2654.

Representative Procedure for the Synthesis of Tetraindole 4: 2,5-Bis(di(1H-indol-3-yl)methyl)thiophene (4). A round-bottomed flask (10 mL) was charged with 2,5-thiophenedicarboxaldehyde (0.14 g, 1.0 mmol), indole (0.47 g, 4 mmol), and iodine (0.025 g, 0.1 mmol) in ether (1 mL). This mixture was then stirred for 2 h at room temperature. The reaction mixture was treated with aqueous $\text{Na}_2\text{S}_2\text{O}_3$, and the solution was extracted with ethyl acetate (2×20 mL). The combined organic layers were dried over MgSO_4 and filtered. The solvent was removed under reduced pressure, and the residue was subjected to flash column chromatography, followed by normal-phase HPLC to afford the pure product as a powder (87%), mp 180–181 °C. ^1H NMR (400 MHz, CDCl_3) 7.41 (d, $J = 7.8$ Hz, 4H), 7.38–7.29 (m, 4H), 7.17–7.10 (m, 8H), 7.01 (td, $J = 6.8, 1.4$ Hz, 4H), 6.63 (s, 2H), 6.37 (m, 4H), 5.95 (s, 2H). ^{13}C NMR (100 MHz, CDCl_3) 146.5, 136.4, 126.7, 124.4, 123.3, 121.8, 119.8, 119.4, 119.1, 111.2, 35.6. HRMS calcd for $\text{C}_{38}\text{H}_{28}\text{N}_4\text{S}$ (M^+), 572.2035; found, 572.2031.

1,4-Bis(di(5-bromo-1H-indol-3-yl)methyl)benzene (5). Yield 75% (powder), mp 195–196 °C. ^1H NMR (300 MHz, CDCl_3) 8.08 (br s, 4H), 7.45 (s, 4H), 7.28–7.18 (m, 8H), 7.10 (s, 4H), 6.40 (s, 4H), 5.65 (s, 2H). ^{13}C NMR (75 MHz, CDCl_3) 141.2, 135.3, 128.0, 125.0, 124.6, 122.1, 118.7, 112.8, 112.3, 39.5. HRMS calcd for $\text{C}_{40}\text{H}_{25}\text{N}_4\text{Br}_4$ ($\text{M} - \text{H}$), 876.8813; found, 876.8817.

Representative Procedure for the Synthesis of Tetraindole 6: 3,3'-(4-Di(1H-indol-3-yl)methyl)phenyl)methylene)bis(5-bromo-1H-indole) (6). A round-bottomed flask (10 mL) was charged with 4-(bis(5-bromo-1H-indol-3-yl)methyl)benzaldehyde 21 (0.25 g, 0.5 mmol), indole (0.12 g, 1 mmol), and iodine (0.012 g, 0.05 mmol) in MeCN (1 mL). The mixture was then stirred for 2 h at room temperature. The reaction mixture was treated with aqueous $\text{Na}_2\text{S}_2\text{O}_3$, and the solution was extracted with ethyl acetate (2×20 mL). The combined organic layers were dried over MgSO_4 and filtered. The solvent was removed under reduced pressure, and the residue was subjected to flash column chromatography, followed by normal-phase HPLC to afford the pure product as a powder (80%), mp 210–211 °C. ^1H NMR (400 MHz, CDCl_3) 7.59 (br s, 2H), 7.46–7.38 (m, 5H), 7.31–7.22 (m, 5H), 7.19–7.12 (m, 6H), 7.09–7.02 (m, 4H), 6.34 (s, 2H), 6.20 (s, 2H), 5.78 (s, 1H), 5.59 (s, 1H). ^{13}C NMR (100 MHz, CDCl_3) 141.7, 140.6, 136.5, 135.0, 128.6, 128.4, 128.3,

126.8, 124.9, 124.5, 123.7, 122.2, 121.8, 119.8, 119.2, 119.0, 118.5, 112.8, 112.2, 111.4, 39.8, 39.4. HRMS calcd for $\text{C}_{40}\text{H}_{28}\text{N}_4\text{Br}_2\text{Na}$ ($\text{M} + \text{Na}$)⁺, 745.0578; found, 745.0595.

1,4-Bis(di(5-cyano-1H-indol-3-yl)methyl)benzene (7). Yield 45% (powder), mp 154–155 °C. ^1H NMR (500 MHz, acetone- d_6) 11.44 (br s, 4H), 7.79 (s, 4H), 7.51 (d, $J = 8.5$ Hz, 4H), 7.38 (m, d, $J = 7.5$ Hz, 4H), 7.32 (s, 4H), 7.12 (s, 4H), 5.99 (s, 2H). ^{13}C NMR (125 MHz, DMSO- d_6) 142.3, 138.7, 128.6, 126.8, 126.7, 125.0, 124.2, 119.5, 113.4, 100.8, 38.6. HRMS calcd for $\text{C}_{44}\text{H}_{26}\text{N}_8\text{Na}$ ($\text{M} + \text{Na}$)⁺, 689.2178; found, 689.2185.

1,4-Bis(di(5-hydroxy-1H-indol-3-yl)methyl)benzene (8). Yield 89% (powder), mp 239–240 °C. ^1H NMR (400 MHz, CD_3OD) 7.24 (s, 4H), 7.13 (d, $J = 8.6$ Hz, 4H), 6.73 (d, $J = 2.3$ Hz, 4H), 6.68–6.58 (m, 8H), 5.63 (s, 2H). ^{13}C NMR (100 MHz, CD_3OD) 150.1, 143.1, 133.0, 129.0, 128.7, 125.2, 119.1, 112.0, 111.6, 104.4, 41.0. HRMS calcd for $\text{C}_{40}\text{H}_{30}\text{N}_4\text{O}_4\text{Na}$ ($\text{M} + \text{Na}$)⁺, 653.2165; found, 653.2171.

1,4-Bis(di(5-methoxy-1H-indol-3-yl)methyl)benzene (9). Yield 70% (powder), mp 257–258 °C. ^1H NMR (400 MHz, DMSO- d_6) 10.60 (br s, 4H), 7.25 (s, 4H), 7.21 (d, $J = 8.6$ Hz, 4H), 6.76 (s, 4H), 6.69–6.65 (m, 8H), 5.69 (s, 2H), 3.52 (s, 12H). ^{13}C NMR (125 MHz, DMSO- d_6) 153.1, 142.7, 132.2, 128.5, 127.5, 124.6, 118.4, 112.5, 111.1, 101.7, 55.6, 39.5. HRMS calcd for $\text{C}_{44}\text{H}_{38}\text{N}_4\text{O}_4$ ($\text{M} +$), 686.2893; found, 686.2876.

Representative Procedure for the Synthesis of Tetraindole 10: 3,3',3'',3'''-(1,4-Phenylenebis(methanetriyl)tetrakis(1H-indol-5-amine)) (10). *Step 1.* A round-bottomed flask (10 mL) was charged with 5-aminoindole (0.66 g, 5.0 mmol), Fmoc-OSu (2.00 g, 6.5 mmol), and triethylamine (1.0 mL, 7.5 mmol) in dichloromethane (30 mL). This mixture was then stirred for 5 h at room temperature. The reaction mixture was treated with dilute HCl solution and extracted with dichloromethane (2×30 mL). The combined organic layers were dried over MgSO_4 and filtered. The solvent was removed under reduced pressure, and the residue was subjected to flash column chromatography to afford the Fmoc-protected 5-aminoindole (80%).

Step 2. A round-bottomed flask (100 mL) was charged with phthalaldehyde (0.067 g, 0.5 mmol), Fmoc-protected 5-aminoindole (0.71 g, 2 mmol), and iodine (0.025 g, 0.1 mmol) in MeCN/DMSO (5 mL). The mixture was then stirred overnight at room temperature. The reaction mixture was treated with $\text{Na}_2\text{S}_2\text{O}_3$ solution, extracted with dichloromethane (2×30 mL). The combined organic layers were dried over MgSO_4 and filtered. The solvent was removed under reduced pressure, and the residue was subjected to flash column chromatography to obtain the protected tetraindole **20** (60%).

Step 3. A round-bottomed flask (100 mL) was charged with the Fmoc protected tetraindole **20** (0.76 g, 0.5 mmol) and DBU (299 μL , 2 mmol) in dichloromethane (50 mL). The mixture was then stirred for 30 min at room temperature. The reaction mixture was treated with $\text{Na}_2\text{S}_2\text{O}_3$ solution and extracted with dichloromethane (2×30 mL). The combined organic layers were dried over MgSO_4 and filtered. The solvent was removed under reduced pressure, and the residue was subjected to flash column chromatography, followed by precipitation from DMSO to afford pure product **10** as a powder (50%), mp 134–135 °C. ^1H NMR (400 MHz, DMSO- d_6) 10.22 (br s, 4H), 7.14 (s, 4H), 7.01 (d, $J = 8.5$ Hz, 4H), 6.53 (d, $J = 2.1$ Hz, 4H), 6.47–6.40 (m, 8H), 5.46 (s, 2H), 4.30 (br s, 8H, NH_2). ^{13}C NMR (125 MHz, DMSO- d_6) 142.4, 140.0, 130.6, 127.8, 127.5, 123.4, 117.2, 111.9, 111.6, 102.8, 39.9. HRMS calcd for $\text{C}_{40}\text{H}_{35}\text{N}_8$ ($\text{M} + \text{H}$)⁺, 627.2985; found, 627.2988.

1,3-Bis(di(5-hydroxy-1H-indol-3-yl)methyl)benzene (11). Yield 85% (powder), mp 285–286 °C. ^1H NMR (400 MHz, CD_3OD) 7.39 (s, 1H), 7.13 (m, 7H), 6.72 (d, $J = 2.4$ Hz, 4H), 6.64 (dd, $J = 8.6, 2.4$ Hz, 4H), 6.49 (s, 4H), 5.60 (s, 2H). ^{13}C NMR (100 MHz, CD_3OD) 150.0, 145.3, 132.9, 130.1, 128.6, 128.2, 126.9, 125.2, 118.9, 112.0, 111.6, 104.4, 41.3. HRMS calcd for $\text{C}_{40}\text{H}_{31}\text{N}_4\text{O}_4$ ($\text{M} + \text{H}$)⁺, 631.2345; found, 631.2332.

3,3',3'',3'''-(1,4-Phenylenebis(methanetriyl)tetrakis(1H-indol-6-ol)) (12). Yield 55% (powder), mp >300 °C. ^1H NMR (400 MHz, CD_3OD) 7.22 (s, 4H), 7.05 (d, $J = 8.5$ Hz, 4H), 6.73 (s, 4H),

6.48–6.44 (m, 8H), 5.66 (s, 2H). ¹³C NMR (100 MHz, CD₃OD) 153.0, 143.2, 138.7, 128.9, 122.8, 122.2, 120.6, 119.8, 109.0, 97.0, 40.9. HRMS calcd for C₄₀H₃₅N₄O₄ (M + H)⁺, 631.2345; found, 631.2340.

Representative Procedure for the Synthesis of Tetraindole 13: 3-(4-Di(1H-indol-3-yl)methyl)phenyl(1H-indol-3-yl)methyl(1H-indol-5-ol) (13). A round-bottomed flask (10 mL) was charged with terephthalaldehyde (0.13 g, 1.0 mmol), indole (0.28 g, 2.4 mmol), 5-hydroxyindole (0.21 g, 1.6 mmol), and iodine (0.025 g, 0.1 mmol) in MeCN (1 mL). The mixture was then stirred for 2 h at room temperature. The reaction mixture was treated with Na₂S₂O₃ solution and extracted with ethyl acetate (2 × 20 mL). The combined organic layers were dried over MgSO₄ and filtered. The solvent was removed under reduced pressure, and the residue was subjected to flash column chromatography, followed by normal-phase HPLC to afford the pure product as a powder (30%), mp 139–140 °C. ¹H NMR (500 MHz, acetone-*d*₆) 9.94 (br s, 3H), 9.67 (br s, 1H), 7.54 (br s, 1H), 7.37–7.33 (m, 10H), 7.19 (d, *J* = 8.5 Hz, 1H), 7.06 (t, *J* = 8.0 Hz, 3H), 6.90 (t, *J* = 7.5 Hz, 3H), 6.38–6.66 (m, 6H), 5.91 (s, 1H), 5.80 (s, 1H). ¹³C NMR (100 MHz, CD₃OD) 151.3, 143.5, 143.4, 138.1, 132.9, 129.2, 129.2, 128.9, 128.3, 128.2, 125.2, 124.6, 124.5, 122.0, 122.0, 120.4, 120.4, 120.2, 120.1, 119.4, 119.3, 119.3, 112.5, 112.3, 112.2, 112.1, 104.6, 40.9, 40.9. HRMS calcd for C₄₀H₃₀N₄O₄Na (M + Na)⁺, 605.2317; found, 605.2324.

Representative Procedure for the Synthesis of Tetraindole 14: 3,3'-(4-Di(1H-indol-3-yl)methyl)phenylmethylenebis(1H-indol-5-ol) (14). *Step 1.* A round-bottomed flask (10 mL) was charged with terephthalaldehyde (0.13 g, 1.0 mmol), indole (0.23 g, 2 mmol), and iodine (0.012 g, 0.05 mmol) in ether (1 mL). The mixture was then stirred for 15 min at room temperature. The reaction mixture was treated with Na₂S₂O₃ solution and extracted with ethyl acetate (2 × 20 mL). The combined organic layers were dried over MgSO₄ and filtered. The solvent was removed under reduced pressure, and the residue was subjected to flash column chromatography to give 4-(bis(1H-indol-3-yl)methyl)benzaldehyde **22** (67%).

Step 2. A round-bottomed flask (10 mL) was charged with **22** (0.18 g, 0.5 mmol), indole (0.12 g, 1 mmol), and iodine (0.012 g, 0.05 mmol) in MeCN (1 mL). The mixture was then stirred for 15 min at room temperature. The reaction mixture was treated with Na₂S₂O₃ solution and extracted with ethyl acetate (2 × 20 mL). The combined organic layers were dried over MgSO₄ and filtered. The solvent was removed under reduced pressure, and the residue was subjected to flash column chromatography, followed by normal-phase HPLC to afford the pure product as a powder (60%), mp 174–175 °C. ¹H NMR (400 MHz, acetone-*d*₆) 9.92 (br s, 2H), 9.65 (br s, 2H), 7.59 (br s, 2H, OH), 7.37–7.30 (m, 8H), 7.19 (d, *J* = 9.0 Hz, 2H), 7.05 (t, *J* = 7.5 Hz, 2H), 6.90 (t, *J* = 8.0 Hz, 2H), 6.82 (d, *J* = 1.5 Hz, 2H), 6.77 (d, *J* = 2.0 Hz, 2H), 6.68–6.66 (m, 4H), 5.90 (s, 1H), 5.60 (s, 1H). ¹³C NMR (100 MHz, acetone-*d*₆) 151.2, 143.4, 143.3, 138.0, 132.8, 129.2, 129.1, 128.9, 128.2, 125.2, 124.5, 122.0, 120.4, 120.1, 119.3, 119.2, 112.5, 112.2, 112.1, 104.5, 40.9, 40.9. HRMS calcd for C₄₀H₃₀N₄O₂Na (M + Na)⁺, 621.2266; found, 621.2252.

Representative Procedure for the Synthesis of Tetraindole 15: 3,3'-(4-Di(5-hydroxy-1H-indol-3-yl)(1H-indol-3-yl)methyl)phenylmethylenebis(1H-indol-5-ol) (15). A round-bottomed flask (10 mL) was charged with terephthalaldehyde (0.13 g, 1.0 mmol), indole (0.094 g, 0.8 mmol), 5-hydroxyindole (0.43 g, 3.2 mmol), and iodine (0.025 g, 0.1 mmol) in MeCN (1 mL). The mixture was then stirred for 2 h at room temperature. The reaction mixture was treated with Na₂S₂O₃ solution and extracted with ethyl acetate (2 × 20 mL). The combined organic layers were dried over MgSO₄ and filtered. The solvent was removed under reduced pressure, and the residue was subjected to flash column chromatography, followed by normal-phase HPLC to afford the pure product as a powder (60%), mp 228–229 °C. ¹H NMR (500 MHz, acetone-*d*₆) 9.94 (br s, 1H), 9.68 (br s, 3H), 7.54 (br s, 3H, OH), 7.38–7.36 (m, 2H), 7.34–7.30 (m, 4H), 7.20 (dd, *J* = 8.5 Hz, 1 Hz, 3H), 7.06 (t, *J* = 7.5 Hz, 1H), 6.91 (t, *J* = 7.7 Hz, 1H), 6.81 (d, *J* = 1.5 Hz, 1H), 6.76–6.74 (m, 4H), 6.72–6.70 (m, 2H), 6.67–6.65 (m, 3H), 5.79 (s, 1H), 5.67 (s, 1H). ¹³C NMR (100 MHz, CD₃OD) 151.2, 143.4, 143.4,

138.1, 132.9, 129.2, 129.2, 128.9, 128.9, 128.2, 125.2, 124.6, 122.0, 120.4, 120.17, 119.3, 112.5, 112.3, 112.2, 112.1, 104.6, 104.5, 41.0, 41.0. HRMS calcd for C₄₀H₃₁N₄O₃ (M + H)⁺, 615.2396; found, 615.2400.

Biology. Cell viability analysis²⁷ and fluorescence microscopy analysis²⁸ were performed by employing previously described methods.

Cell Culture. Human breast carcinoma cell line MCF-7 and human adenocarcinoma cells MDA-MB-231 (BCRC-60436; BCRC-60425, Bioresource Collection and Research Center, Food Industry Research and Development Institute, Hsinchu, Taiwan) were maintained in Dulbecco's Modified Eagle's medium (DMEM) containing 10% fetal bovine serum (FBS) and 2 mM L-glutamine at 37 °C in a humidified atmosphere containing 5% CO₂ in air.

Cell Growth Inhibition Analysis. MDA-MB-231 cells were seeded at a density of 2 × 10⁵ per well in 6-well culture plates. After 24 h, cells were treated with different concentrations of **8** or DMSO (vehicle control) in triplicates. At different time intervals, cells were harvested by trypsinization, stained with 0.4% trypan blue, and counted using a hemocytometer.

Flow Cytometry Analysis. Cells were incubated in 10% FBS-supplemented DMEM/F12 with DMSO (vehicle control) or different concentrations of **8** for 24 h. After treatment, cells were collected by trypsinization and centrifugation, washed with PBS, and fixed with ice-cold 70% ethanol at –20 °C overnight. Fixed cells were collected by centrifugation, washed with PBS, resuspended in 0.5 mL of PBS containing 20 μg/mL propidium iodide, 200 μg/mL RNase A, and 0.1% triton X-100. Samples were incubated on the ice and kept in the dark for 30 min. The cell cycle distribution was analyzed by using a FACSCalibur flow cytometer (BD), and the ranges for G₁, S, G₂/M, and sub-G₁ phase cells were validated according to the corresponding DNA contents, followed by calculated using ModFIT LT software (BD).

Determination of the Apoptotic DNA Ladder. MDA-MB-231 cells were seeded at a density of 1 × 10⁶ per well in 10 cm² culture dishes. After 24 h, cells were treated with different concentration of **8** or DMSO (vehicle control) and then incubated in 37 °C, 5% CO₂ incubator for 48 h. After treatment, the attached and suspension cells were harvested by trypsinization and centrifugation. The pellets were washed twice using PBS and lysed in TE lysis buffer (10 mM Tris-HCl pH 7.5, 1 mM sodium-EDTA, 0.25% NP40). The supernatants were collected and incubated with 5 μL of RNase A (20 mg/mL) for 1 h at 37 °C, followed by adding 5 μL of proteinase K (20 mg/mL) for 1 h at 37 °C. The electrophoresis was performed with 1.8% agarose gel.

Protein Extraction and Western Blot Analysis. MDA-MB-231 cells were treated with 0.2, 0.4, 0.8 μM **8** for 24 and 48 h. After treatment, the suspended and attached cells were collected by trypsinization and centrifugation and lysed in lysis buffer (25 mM Tris-HCl, pH 7.6, 150 mM NaCl, 0.1% SDS, 1% NP-40, 1% sodium deoxycholate) with proteinase inhibitors. The lysates were incubated on ice for 10 min and centrifuged at 13000g for 20 min. Protein concentrations were then determined with BCA protein assay reagents (Pierce). Equal amounts of total protein were mixed with 4× sample loading buffer (62.5 mM Tris-HCl pH 6.8, 10% glycerol, 20% SDS, 2.5% bromophenol blue, and 5% 2-mercaptoethanol), boiled for 10 min, and then fractionated by electrophoresis on 10% and 15% SDS-PAGE. Prestained protein ladder (Fermentas) was used as the molecular weight standard. Proteins were electrically transferred to nitrocellulose membranes and blocked overnight at 4 °C with 0.05% TBST and 5% nonfat milk. Blots were subsequently incubated for 1 h at room temperature for phospho-cdc2 (Santa Cruz), caspase-3 (IMGENEX), cyclin B1 (Cell Signaling), bak/bcl-2 (AbD), and actin (Chemicon) primary antibodies. Immunoreactive proteins were detected after incubation with horseradish peroxidase-conjugated secondary antibody. The immunoblots were visualized by enhanced chemiluminescence.

■ ASSOCIATED CONTENT

■ Supporting Information

Details of HPLC, ¹H and ¹³C NMR spectra of all new tetraindols, and effect of **8** on the viability of MDA-MB-231 cells. This material is available free of charge via the Internet at <http://pubs.acs.org>.

■ AUTHOR INFORMATION

Corresponding Author

*For W.-S.L.: phone, +886 (2) 27898662; fax, +886 (2) 27831237; e-mail, wenshan@chem.sinica.edu.tw. For C.-F.Y.: phone, +886 (2) 77346128; fax, +886 (2) 29324249; e-mail, cheyao@ntnu.edu.tw.

Present Address

#These authors contributed equally to this work.

Notes

The authors declare no competing financial interest.

■ ACKNOWLEDGMENTS

We are grateful for funding of this work provided by the Academia Sinica and the National Science Council. Instrumentation support was provided by the NMR and Mass Spectrometry facilities of the Institute of Chemistry at Academia Sinica, Taiwan.

■ ABBREVIATIONS USED

I3C, indole-3-carbinol; cdk1, cdc2 kinase; cPARP, cleavage of poly(ADP-ribose)polymerase; PS, phosphatidylserine; ER, estrogen receptor; ROS, reactive oxygen species; JNK, c-Jun N-terminal kinase; IC₅₀, inhibitory concentration 50%; MTT, 3-(4,5-dimethylthiazol-2-yl)-2,5-diphenyl tetrazolium bromide

■ REFERENCES

(1) (a) Aronchik, I.; Bjeldanes, L. F.; Firestone, G. L. Direct inhibition of elastase activity by indole-3-carbinol triggers a CD40-TRAF regulatory cascade that disrupts NF- κ B transcriptional activity in human breast cancer cells. *Cancer Res.* **2010**, *70*, 4961–4971. (b) Melkamu, T.; Zhang, X.; Tan, J.; Zeng, Y.; Kassie, F. Alteration of microRNA expression in vinyl carbamate-induced mouse lung tumors and modulation by the chemopreventive agent indole-3-carbinol. *Carcinogenesis* **2010**, *31*, 252–258. (c) Safe, S.; Papineni, S.; Chintharlapalli, S. Cancer chemotherapy with indole-3-carbinol, bis(3'-indolyl)methane and synthetic analogs. *Cancer Lett.* **2008**, *269*, 326–338. and references therein. (d) Weng, J. R.; Tsai, C. H.; Kulp, S. K.; Chen, C. S. Indole-3-carbinol as a chemopreventive and anti-cancer agent. *Cancer Lett.* **2008**, *262*, 153–163. and references therein. (e) Nguyen, H. H.; Aronchik, I.; Brar, G. A.; Nguyen, D. H.; Bjeldanes, L. F.; Firestone, G. L. The dietary phytochemical indole-3-carbinol is a natural elastase enzymatic inhibitor that disrupts cyclin E protein processing. *Proc. Natl. Acad. Sci. U.S.A.* **2008**, *105*, 19750–19755. (2) (a) Rajoria, S.; Suriano, R.; George, A.; Shanmugam, A.; Schantz, S. P.; Geliebter, J.; Tiwari, R. K. Estrogen induced metastatic modulators MMP-2 and MMP-9 are targets of 3,3'-diindolylmethane in thyroid cancer. *PLoS One* **2011**, *6*, e15879. (b) Kandala, P. K.; Srivastava, S. K. Activation of checkpoint kinase 2 by 3,3'-diindolylmethane is required for causing G2/M cell cycle arrest in human ovarian cancer cells. *Mol. Pharmacol.* **2010**, *78*, 297–309. (c) Li, Y.; Li, X.; Guo, B. Chemopreventive agent 3,3'-diindolylmethane selectively induces proteasomal degradation of class I histone deacetylases. *Cancer Res.* **2010**, *70*, 646–654. (d) Fan, S.; Meng, Q.; Saha, T.; Sarkar, F. H.; Rosen, E. M. Low concentrations of diindolylmethane, a metabolite of indole-3-carbinol, protect against oxidative stress in a BRCA1-dependent manner. *Cancer Res.* **2009**, *69*, 6083–6091. (e) Bhuiyan, M. M.; Li, Y.; Banerjee, S.; Ahmed, F.; Wang, Z.; Ali, S.; Sarkar, F. H.

Down-regulation of androgen receptor by 3,3'-diindolylmethane contributes to inhibition of cell proliferation and induction of apoptosis in both hormone-sensitive LNCaP and insensitive C4-2B prostate cancer cells. *Cancer Res.* **2006**, *66*, 10064–10072.

(3) (a) Xue, L.; Schaldach, C. M.; Janosik, T.; Bergman, J.; Bjeldanes, L. F. Effects of analogs of indole-3-carbinol cyclic trimerization product in human breast cancer cells. *Chem. Biol. Interact.* **2005**, *152*, 119–129. (b) Riby, J. E.; Feng, C.; Chang, Y. C.; Schaldach, C. M.; Firestone, G. L.; Bjeldanes, L. F. The major cyclic trimeric product of indole-3-carbinol is a strong agonist of the estrogen receptor signaling pathway. *Biochemistry* **2000**, *39*, 910–918.

(4) (a) De Santi, M.; Galluzzi, L.; Lucarini, S.; Paoletti, M. F.; Fraternali, A.; Duranti, A.; De Marco, C.; Fanelli, M.; Zaffaroni, N.; Brandi, G.; Magnani, M. The indole-3-carbinol cyclic tetrameric derivative CTet inhibits cell proliferation via overexpression of p21/CDKN1A in both estrogen receptor-positive and triple-negative breast cancer cell lines. *Breast Cancer Res.* **2011**, *13*, R33. (b) Lucarini, S.; De Santi, M.; Antonietti, F.; Brandi, G.; Diamantini, G.; Fraternali, A.; Paoletti, M. F.; Tontini, A.; Magnani, M.; Duranti, A. Synthesis and biological evaluation of a gamma-cyclodextrin-based formulation of the anticancer agent 5,6,11,12,17,18,23,24-octahydrocyclododeca[1,2-b:4,5-b':7,8-b'':10,11-b''']tetraindole (CTet). *Molecules* **2010**, *15*, 4085–4093. (c) Brandi, G.; Paiardini, M.; Cervasi, B.; Fiorucci, C.; Filippone, P.; De Marco, C.; Zaffaroni, N.; Magnani, M. A new indole-3-carbinol tetrameric derivative inhibits cyclin-dependent kinase 6 expression, and induces G1 cell cycle arrest in both estrogen-dependent and estrogen-independent breast cancer cell lines. *Cancer Res.* **2003**, *63*, 4028–4036.

(5) NCI, DCPC Chemoprevention Branch and Agent Development Committee. Clinical Development Plan: Indole-3-carbinol. *J. Cell. Biochem.* **1996**, *26*, 127–136.

(6) (a) Wang, Z.; Yu, B. W.; Rahman, K. M.; Ahmad, F.; Sarkar, F. H. Induction of growth arrest and apoptosis in human breast cancer cells by 3,3'-diindolylmethane is associated with induction and nuclear localization of p27kip. *Mol. Cancer Ther.* **2008**, *7*, 341–349. (b) Vanderlaag, K.; Samudio, I.; Burghardt, R.; Barhoumi, R.; Safe, S. Inhibition of breast cancer cell growth and induction of cell death by 1,1-bis(3'-indolyl)methane (DIM) and 5,5'-dibromoDIM. *Cancer Lett.* **2006**, *236*, 198–212. (c) Meng, Q.; Qi, M.; Chen, D. Z.; Yuan, R.; Goldberg, I. D.; Rosen, E. M.; Auburn, K.; Fan, S. Suppression of breast cancer invasion and migration by indole-3-carbinol: associated with up-regulation of BRCA1 and E-cadherin/catenin complexes. *J. Mol. Med. (Berlin)* **2000**, *78*, 155–165.

(7) (a) Ahmad, A.; Sakr, W. A.; Rahman, K. M. Anticancer properties of indole compounds: mechanism of apoptosis induction and role in chemotherapy. *Curr. Drug Targets.* **2010**, *11*, 652–666. and references therein. (b) Rahman, K. W.; Sarkar, F. H. Inhibition of nuclear translocation of nuclear factor- κ B contributes to 3,3'-diindolylmethane-induced apoptosis in breast cancer cells. *Cancer Res.* **2005**, *65*, 364–371. (c) Sarkar, F. H.; Rahman, K. M.; Li, Y. Bax translocation to mitochondria is an important event in inducing apoptotic cell death by indole-3-carbinol (I3C) treatment of breast cancer cells. *J. Nutr.* **2003**, *133*, 2434S–2439S.

(8) Anderton, M. J.; Manson, M. M.; Verschoyle, R. D.; Gescher, A.; Lamb, J. H.; Farmer, P. B.; Steward, W. P.; Williams, M. L. Pharmacokinetics and tissue disposition of indole-3-carbinol and its acid condensation products after oral administration to mice. *Clin. Cancer Res.* **2004**, *10*, 5233–5241.

(9) (a) Tung, Y. S.; Coumar, M. S.; Wu, Y. S.; Shiao, H. Y.; Chang, J. Y.; Liou, J. P.; Shukla, P.; Chang, C. W.; Chang, C. Y.; Kuo, C. C.; Yeh, T. K.; Lin, C. Y.; Wu, J. S.; Wu, S. Y.; Liao, C. C.; Hsieh, H. P. Scaffold-hopping strategy: synthesis and biological evaluation of 5,6-fused bicyclic heteroaromatics to identify orally bioavailable anticancer agents. *J. Med. Chem.* **2011**, *54*, 3076–3080. (b) Kuo, C. C.; Hsieh, H. P.; Pan, W. Y.; Chen, C. P.; Liou, J. P.; Lee, S. J.; Chang, Y. L.; Chen, L. T.; Chen, C. T.; Chang, J. Y. BPROL075, a novel synthetic indole compound with antimetabolic activity in human cancer cells, exerts effective antitumoral activity in vivo. *Cancer Res.* **2004**, *64*, 4621–4628.

- (10) (a) Ahn, S.; Kearbey, J. D.; Li, C. M.; Duke, C. B. III; Miller, D. D.; Dalton, J. T. Biotransformation of a novel antimetabolic agent, I-387, by mouse, rat, dog, monkey, and human liver microsomes and in vivo pharmacokinetics in mice. *Drug Metab. Dispos.* **2011**, *39*, 636–643. (b) Ahn, S.; Duke, C. B. III; Barrett, C. M.; Hwang, D. J.; Li, C. M.; Miller, D. D.; Dalton, J. T. I-387, a novel antimetabolic indole, displays a potent in vitro and in vivo antitumor activity with less neurotoxicity. *Mol. Cancer Ther.* **2010**, *9*, 2859–2868.
- (11) (a) Guo, W.; Wei, X.; Wu, S.; Wang, L.; Peng, H.; Wang, J.; Fang, B. Antagonistic effect of flavonoids on NSC-741909-mediated antitumor activity via scavenging of reactive oxygen species. *Eur. J. Pharmacol.* **2010**, *649*, 51–58. (b) Wei, X.; Guo, W.; Wu, S.; Wang, L.; Lu, Y.; Xu, B.; Liu, J.; Fang, B. Inhibiting JNK dephosphorylation and induction of apoptosis by novel anticancer agent NSC-741909 in cancer cells. *J. Biol. Chem.* **2009**, *284*, 16948–16955.
- (12) Chao, W. R.; Yean, D.; Amin, K.; Green, C.; Jong, L. Computer-aided rational drug design: a novel agent (SR13668) designed to mimic the unique anticancer mechanisms of dietary indole-3-carbinol to block Akt signaling. *J. Med. Chem.* **2007**, *50*, 3412–3415.
- (13) Ohkubo, M.; Nishimura, T.; Honma, T.; Nishimura, I.; Ito, S.; Yoshinari, T.; Suda, H. A.; Morishima, H.; Nishimura, S. Synthesis and biological activities of NB-506 analogues: effects of the positions of two hydroxyl groups at the indole rings. *Bioorg. Med. Chem. Lett.* **1999**, *9*, 3307–3312.
- (14) Weng, J. R.; Tsai, C. H.; Omar, H. A.; Sargeant, A. M.; Wang, D.; Kulp, S. K.; Shapiro, C. L.; Chen, C. S. OSU-A9, a potent indole-3-carbinol derivative, suppresses breast tumor growth by targeting the Akt-NF- κ B pathway and stress response signaling. *Carcinogenesis* **2009**, *30*, 1702–1709.
- (15) Yan, C.; Shieh, B.; Reigan, P.; Zhang, Z.; Colucci, M. A.; Chilloux, A.; Newsome, J. J.; Siegel, D.; Chan, D.; Moody, C. J.; Ross, D. Potent activity of indolequinones against human pancreatic cancer: identification of thioredoxin reductase as a potential target. *Mol. Pharmacol.* **2009**, *76*, 163–172.
- (16) Skibo, E. B.; Xing, C.; Dorr, R. T. Aziridinyl quinone antitumor agents based on indoles and cyclopent[b]indoles: structure–activity relationships for cytotoxicity and antitumor activity. *J. Med. Chem.* **2001**, *44*, 3545–3562.
- (17) Kobayashi, E.; Okamoto, A.; Asada, M.; Okabe, M.; Nagamura, S.; Asai, A.; Saito, H.; Gomi, K.; Hirata, T. Characteristics of antitumor activity of KW-2189, a novel water-soluble derivative of duocarmycin, against murine and human tumors. *Cancer Res.* **1994**, *54*, 2404–2410.
- (18) Lee, C. H.; Yao, C. F.; Huang, S. M.; Ko, S.; Tan, Y. H.; Lee-Chen, G. J.; Wang, Y. C. Novel 2-step synthetic indole compound 1,1,3-tri(3-indolyl)cyclohexane inhibits cancer cell growth in lung cancer cells and xenograft models. *Cancer* **2008**, *113*, 815–825.
- (19) Huang, S. M.; Hsu, P. C.; Chen, M. Y.; Li, W. S.; More, S. V.; Lu, K. T.; Wang, Y. C. The novel indole compound SK228 induces apoptosis and FAK/Paxillin disruption in tumor cell lines and inhibits growth of tumor graft in the nude mouse. *Int. J. Cancer.* **2011**, doi: 10.1002/ijc.26401.
- (20) Ko, S.; Lin, C.; Tu, Z.; Wang, Y. F.; Wang, C. C.; Yao, C. F. CAN and iodine-catalyzed reaction of indole or 1-methylindole with α,β -unsaturated ketone or aldehyde. *Tetrahedron Lett.* **2006**, *47*, 487–492.
- (21) (a) Sampson, J. J. Determination of the resistance of leukocytes. *Arch. Int. Med.* **1924**, *34*, 490–502. (b) Schrek, R. A method for counting the viable cells in normal and in malignant cell suspensions. *Am. J. Cancer* **1936**, *28*, 389–392.
- (22) (a) Touny, L. H.; Banerjee, P. P. Identification of both Myt-1 and Wee-1 as necessary mediators of the p21-independent inactivation of the cdc-2/cyclin B1 complex and growth inhibition of TRAMP cancer cells by genistein. *Prostate* **2006**, *66*, 1542–1555. (b) Hagting, A.; Karlsson, C.; Clute, P.; Jackman, M.; Pines, J. MPF localization is controlled by nuclear export. *EMBO J.* **1998**, *17*, 4127–4138.
- (23) Clarke, P. R.; Leiss, D.; Pagano, M.; Karsenti, E. Cyclin A- and cyclin B-dependent protein kinases are regulated by different mechanisms in *Xenopus* egg extracts. *EMBO J.* **1992**, *11*, 1751–1761.
- (24) (a) Ray, S.; Mohan, R.; Singh, J. K.; Samantaray, M. K.; Shaikh, M. M.; Panda, D.; Ghosh, P. Anticancer and antimicrobial metal-organic pharmaceutical agents based on palladium, gold, and silver N-heterocyclic carbene complexes. *J. Am. Chem. Soc.* **2007**, *129*, 15042–15053. (b) Garrett, M. D. Cell cycle control and cancer. *Curr. Sci.* **2001**, *81*, 515–522. (c) Liu, F.; Rothblum-Oviatt, C.; Ryan, C. E.; Piwnicka-Worms, H. Overproduction of human Myt1 kinase induces a G2 cell cycle delay by interfering with the intracellular trafficking of Cdc2-cyclin B1 complexes. *Mol. Cell. Biol.* **1999**, *19*, 5113–5123.
- (25) Fulda, S.; Debatin, K. M. Extrinsic versus intrinsic apoptosis pathways in anticancer chemotherapy. *Oncogene* **2006**, *25*, 4798–4811.
- (26) Gulmann, C.; Espina, V.; Petricoin, E. III; Longo, D. L.; Santi, M.; Knutsen, T.; Raffeld, M.; Jaffe, E. S.; Liotta, L. A.; Feldman, A. L. Proteomic analysis of apoptotic pathways reveals prognostic factors in follicular lymphoma. *Clin. Cancer Res.* **2005**, *11*, 5847–5855.
- (27) (a) Chang, T. T.; More, S. V.; Lu, I. H.; Hsu, J. C.; Chen, T. J.; Jen, Y. C.; Lu, C. K.; Li, W. S. Isomallyngamide A, A-1 and their analogs suppress cancer cell migration in vitro. *Eur. J. Med. Chem.* **2011**, *46*, 3810–3819. (b) Chang, T. T.; More, S. V.; Lu, N.; Jhuo, J. W.; Chen, Y. C.; Jao, S. C.; Li, W. S. Polyfluorinated bipyridine cisplatin manipulate cytotoxicity through the induction of S-G(2)/M arrest and partial intercalation mechanism. *Bioorg. Med. Chem.* **2011**, *19*, 4887–4894. (c) Chen, J. Y.; Tang, Y. A.; Huang, S. M.; Juan, H. F.; Wu, L. W.; Sun, Y. C.; Wang, S. C.; Wu, K. W.; Balraj, G.; Chang, T. T.; Li, W. S.; Cheng, H. C.; Wang, Y. C. A novel sialyltransferase inhibitor suppresses FAK/paxillin signaling and cancer angiogenesis and metastasis pathways. *Cancer Res.* **2011**, *71*, 473–483. (d) Chiang, C. H.; Wang, C. H.; Chang, H. C.; More, S. V.; Li, W. S.; Hung, W. C. A novel sialyltransferase inhibitor AL10 suppresses invasion and metastasis of lung cancer cells by inhibiting integrin-mediated signaling. *J. Cell Physiol.* **2010**, *223*, 492–499.
- (28) (a) Wang, C. H.; Shih, W. C.; Chang, H. C.; Kuo, Y. Y.; Hung, W. C.; Ong, T. G.; Li, W. S. Preparation and characterization of amino-linked heterocyclic carbene palladium, gold, and silver complexes and their use as anticancer agents that act by triggering apoptotic cell death. *J. Med. Chem.* **2011**, *54*, 5245–5249.